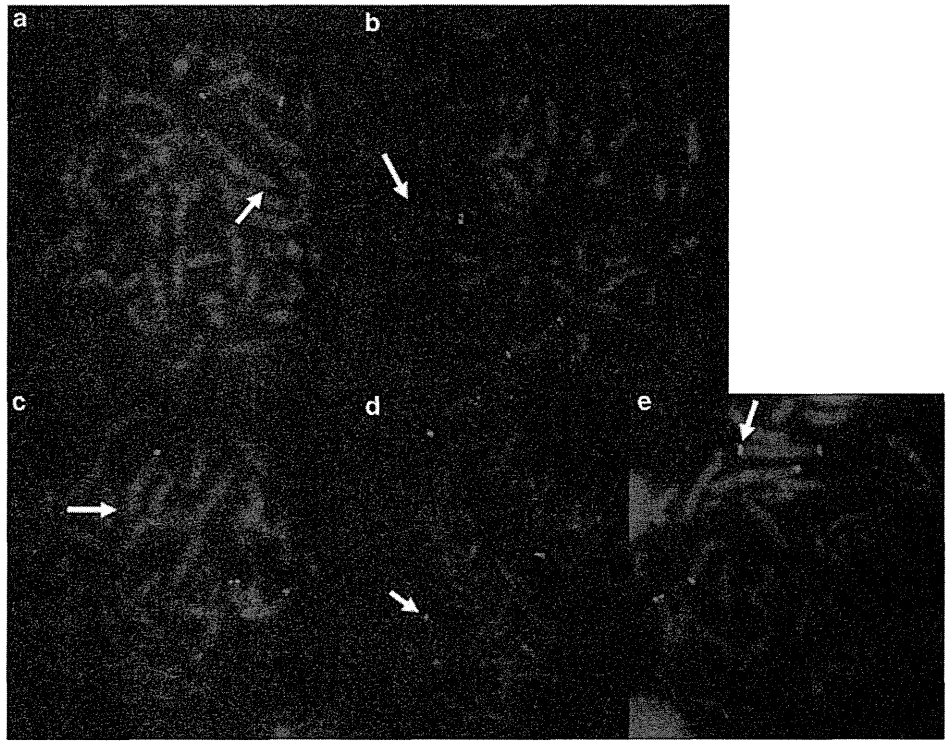

Figure 2 Results of FISH analyses. (**a**) Loss of the green signal labeling RP11-7L23 (arrow) indicates deletion of 1q44 in patient 1. (**b**) Loss of the green signal labeling RP11-88N11 (arrow) indicates deletion of 1q44 in patient 3. (**c–e**) Confirmation of the unbalanced translocation between chromosome 1 and 5 in patient 4. Loss of the green signal labeling RP11-143E8 (arrow) indicates deletion of 1q44 (**c**). An additional signal labeling RP11-94J21 of 5p15.33 is present on the other chromosome (**d**, red signal, arrow), indicating a translocation onto chromosome 1 (**e**, green signal, arrow).

The result of FISH analysis were summarized in Supplementary Table 1.

CLINICAL REPORT

Patient 1

A 9-year-old boy was born by vacuum extraction. His birth weight was 2820 g (within 25th centile), length was 45 cm (= 3rd centile) and occipitofrontal circumference (OFC) was 32.5 cm (10–25th centile). After birth, he displayed feeding problem. His development was mildly delayed with head control attained at 8 months, sitting without support at 15 months, crawling at 24 months and walking alone without support at 44 months. At the age of 11 months, he experienced recurrent febrile seizures. At 18 months of age, he suffered non-febrile seizures. The brain magnetic resonance imaging (MRI) at 4 years of age revealed loss of volume in the frontal lobe, mild abnormal gyral patterns in the frontal lobe and lateral lobe, and ACC (Figures 3a–c). Conventional chromosomal analysis revealed a normal male karyotype.

At present, his height is 119.5 cm (<3rd centile) and weight is 23.6 kg (10th centile). He exhibits microcephaly with OFC of 47.5 cm (<3rd centile). He displays distinctive facial features including a flat occipit, coarse face, high nasal bridge, low-set ears and prominent jaw (Figure 4a). He has short tapering fingers and single palmer creases.

Patient 2

A 3-year and 1-month-old girl is a second child of healthy non-consanguineous parents with an unremarkable family history. She was born at 36th week of gestation after an uneventful pregnancy. She displayed prenatal growth retardation with her weight of 2348 g (<3rd centile), length of 44.4 cm (<3rd centile) and OFC of 31 cm (<3rd centile). At the age of 6 months, developmental delay and microcephaly were noted. She could balance her head at 6 months, sit at 10 months, roll over at 13 months and crawl at 20 months. At the age of 11 months, she suffered febrile convulsion, followed by 11 recurrent attacks of complex febrile seizures. The findings of her electroencephalogram were unremarkable.

At the age of 2 years and 11 months, she had a short stature (height 79 cm, <3rd centile; weight 10 kg, <3rd centile) and microcephaly (OFC 42.5 cm, <3rd centile). Facial dysmorphism included epicanthal folds, a broad nasal root and down-turned corner of mouth (Figure 4b). Neurological examination revealed generalized hypotonia. At this time, she showed moderate psychomotor developmental delay with motor development of 10 months and language development of 8 months. Ultrasonography of the kidneys and liver, echocardiography, ophthalmologic and audiologic examinations revealed no abnormalities. Conventional chromosome analysis revealed a normal female karyotype.

At present, the patient cannot stand without support. She can speak only babbled words. The brain MRI revealed ACC and loss of the volume of the frontal lobe (Figures 3d–f).

Patient 3

A 1-year and 6-month-old girl was born at the gestational age of 38 weeks by vaginal delivery. Although her pregnancy was unremarkable, she showed prenatal growth retardation with her birth weight of 2040 g (<3rd centile) and OFC of 30 cm (<3rd centile). Her APGAR score was 9/9. One hour after birth, she suffered a convulsion

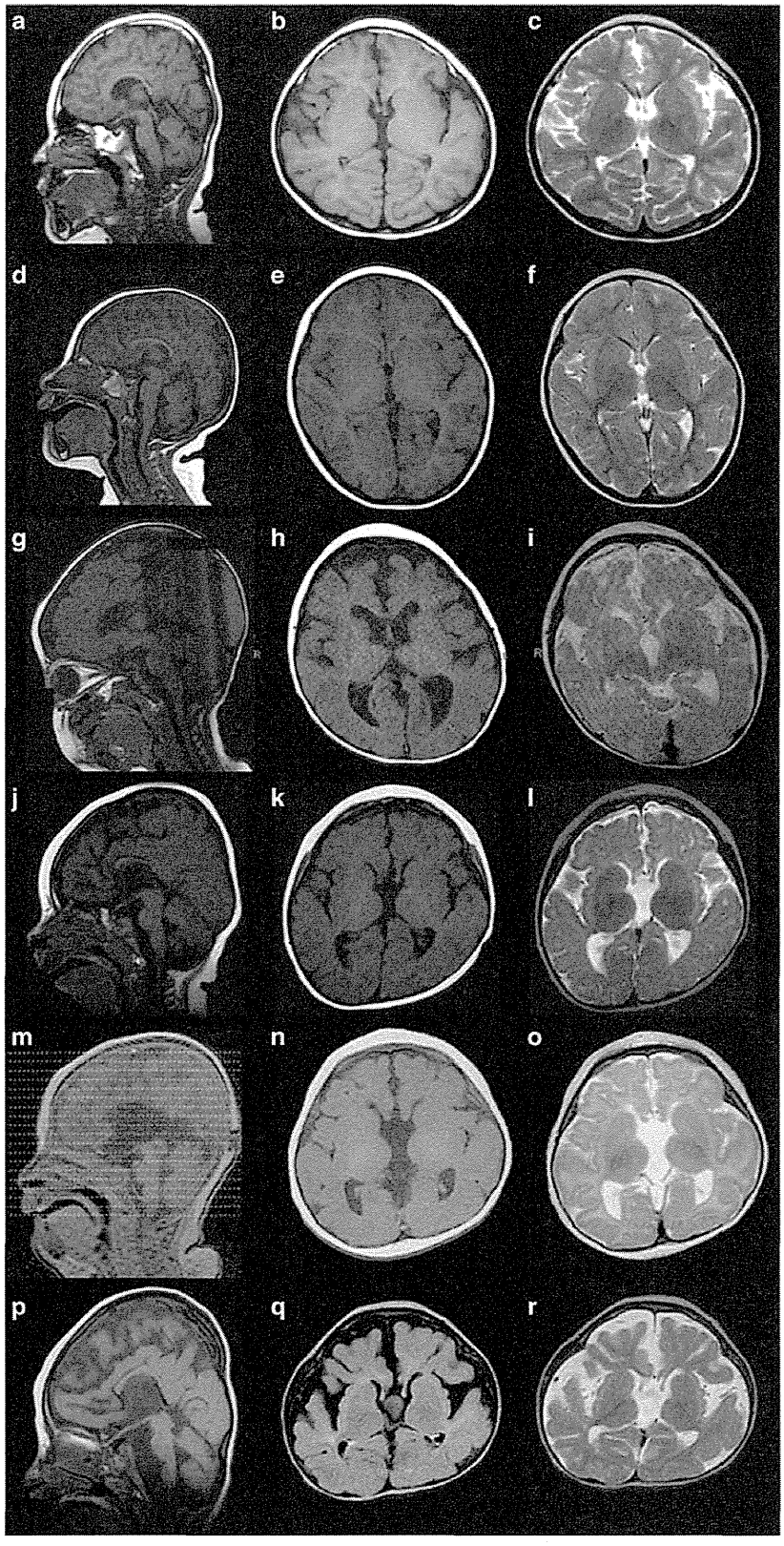

Figure 3 The brain MRI findings of patient 1 examined at 4 years (**a–c**), patient 2 examined at 3 years (**d–f**), patient 3 examined at 12 months (**g–i**), patient 4 examined at 15 months (**j–l**), patient 5 examined at 5 months (**m–o**) and patient 6 examined at 3 years (**p–r**). T1-weighted sagittal views (**a**, **d**, **g**, **j**, **m**, **p**), T1-weighted axial views (**b**, **e**, **h**, **k**, **n**, **q**) and T2-weighted axial views (**c**, **f**, **i**, **l**, **o**, **r**). ACC are noted in all patients. Patient 5 (**m**), in particular, exhibits complete agenesis of the corpus callosum. Reduced volume of the frontal lobe is seen in all patients. Prominently delayed myelination is noted in patient 3 and 4 (**i** and **l**).

triggered by hypoglycemia. Ultrasonography showed enlarged bilateral cerebral ventricles and intraventricular hemorrhage. Echocardiography showed no abnormalities. Ophthalmologic examination displayed exotropia and atrophy of the right retina and optic papilla. Auditory brain-stem response (ABR) showed normal results. Owing to her feeding difficulty, she required tube feeding. At the age of 5 months, she experienced a status convulsive epilepticus, and recurrent spike and waves were noted on EEG at that time. She was treated with several antiepileptic drugs. The brain MRI examined at 1 year of age showed ACC and reduced volume of the brain (Figures 3g–i). Low intensity of the white matter was only noted on the posterior limb of internal capsule, indicating delayed myelination (Figure 3i).

At 1 year and 6 months, the patient could not control her head by herself. She did not demonstrate eye contact, and her feeding difficulties persisted. Distinct facial features included sparse hair, microcephaly, a flat occipit, a coarse face, a high nasal bridge, low-set ears, micrognathia, inversion of eyelids, esotropia and atopic skin. Immediately after this examination, acute respiratory infectious disease caused hypoxic brain damages, which was confirmed by brain computed tomography that revealed the presence of multi-cystic lesions (data not shown). After this event, she shows spastic quadriplegia.

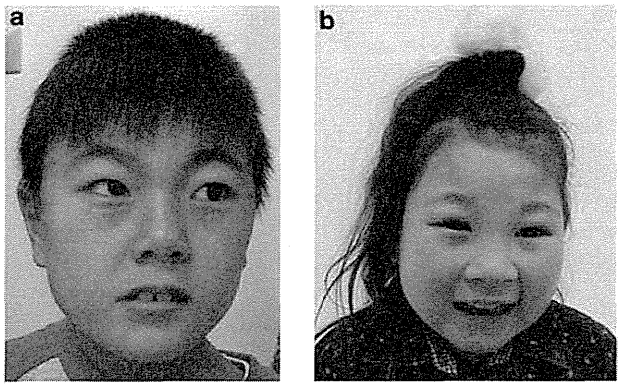

Figure 4 Facial features of patient 1 (**a**) and patient 2 (**b**). Arched eyebrows and small mouth are noted in both patients.

Patient 4

A 3-year and 3-month-old girl was born by induced delivery at 37th week as a first child of healthy, non-consanguineous parents. She showed prenatal growth retardation with her birth weight of 2386 g (<3rd centile), length of 44 cm (<3rd centile) and OFC 31 cm (<3rd centile). Atrial septal defect was revealed by ultrasonography. She displayed psychomotor developmental delay with holding up her head at 5 months, sitting by herself at 14 months and crawling at 20 months. From the age of 14 months, she was prescribed with antiepileptic drugs because of status convulsive that continued for ~1 h. The brain MRI examined at an age of 15 months revealed ACC and hypoplastic brain (Figures 3j–l). Low intensity of the white matter was only noted in the posterior limb of the internal capsule, indicating delayed myelination (Figure 3l). Conventional karyotyping on metaphase spreads prepared from peripheral lymphocytes showed a normal female karyotype.

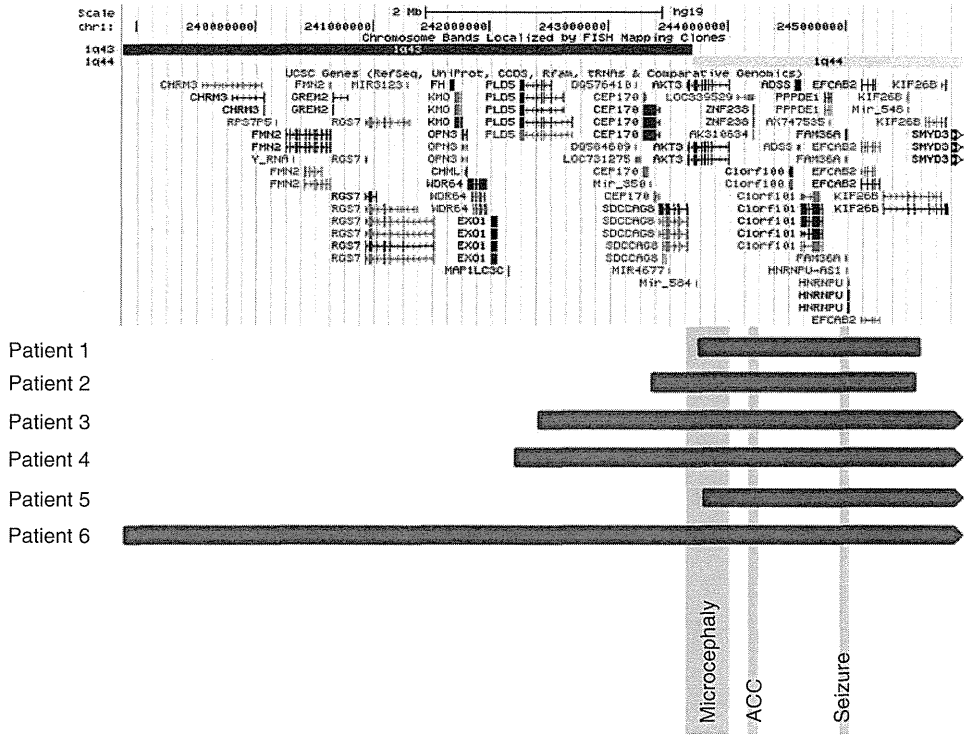

Figure 5 Deletions regions of the present patients depicted on a genome map from UCSC Genome Browser. Blue rectangles indicate the deletion region of the interstitial deletions identified on patients 1 and 2. Blue trapezoids indicate the terminal deletions identified on patients 3–6. Directions of the pointed trapezoids indicate continuous deletions to the telomeres. The region responsible for microcephaly, ACC and seizure that were proposed by Ballif *et al.*[17] are shown by gray rectangles.

Table 1 Summary of the clinical features of six patients in this study

	Patient 1	*Patient 2*	*Patient 3*	*Patient 4*	*Patient 5*	*Patient 6*	*Frequency reported by van Bon et al.*[13]
Karyotype	del (1) (q44q44)	del (1) (q43q44)	del (1) (q43)	del (1) (q43)	del (1) (q44)	del (1) (q43)	
Type of aberrations	Interstitial deletion	Interstitial deletion	Subtelomeric deletion	Unbalanced translocation	Subtelomeric deletion	Subtelomeric deletion	
Deletion region							
Start[a]	243 809 193	243 303 991	242 442 098	242 223 230	243 880 099	238 888 870	
End[a]	245 665 521	245 506 920	249 250 621	249 212 668	249 212 668	249 212 668	
Size (Mb)	1.9	2.2	6.8	7.0	5.3	10.3	
Gender	M	F	F	F	F	F	
Age	9 years	3 years and 1 month	1 year and 6 months	3 years and 3 months	6 years	10 years	
Birth weight (g)	2820	2348	2040	2386	1870	NA	
Controversial points for 1q43 deletions							
Microcephaly	+	+	+	+	+	+	9/11
Abnormalities of the corpus callosum	−	+	+	+	+	+	9/10
Seizures	+	+	+	+	+	+	9/11
Delayed myelination	−	−	+	+	NA	NA	
Severe volume loss of the brain	−	−	+	+	+	+	
General findings							
Developmental delay/mental retardation	+	+	+	+	+	+	11/11
Growth retardation	+	+	NA	+	+	+	7/11
Low birth weight	−	+	+	+	+	NA	5/11
Hypotonia	NA	+	+	NA	+	+	11/11
Feeding problem	+	−	+	−	+	NA	
Facial findings							
Round face	−	+	+	+	NA	NA	7/11
Arched eyebrows	+	+	+	+	NA	NA	
High nasal bridge	+	−	+	−	NA	NA	
Upward-slanting palpebral fissures	+	+	+	+	NA	NA	3/11
Epicanthic folds	+	+	+	+	NA	NA	4/11
Strabismus	+	−	+	−	NA	NA	2/11
Micro/retrognathia	−	−	+	+	NA	NA	0/11
Prominent jaw	+	−	−	−	NA	NA	
Low-set ears	+	+	+	+	NA	NA	
Down-turned corner of mouth	+	+	+	+	NA	NA	
Other features							
Sparse hair	−	−	+	−	NA	NA	
Flat occipit	+	−	+	−	NA	NA	
Tapering fingers	+	−	−	−	NA	NA	
Single palmer creases	+	−	−	−	NA	NA	
Complications of other organs							
Cardiac anomaly	−	−	−	ASD	−	AR	3/11
Kidney/urine pathway anomaly	−	−	−	−	Hydronephrosis	−	2/11

Abbreviations: AR, aortic regurgitation; ASD, atrial septal defect; F, female; M, male; NA, not available.
[a]Genomic positions refer to build 19.

At present, the patient exhibits severe developmental delay as she cannot stand without support and her language usage is limited to babbled words. Her mental and psychomotor developmental index of the Bayley Scales of Infant Development (II) indicate 6 and 8 months, respectively. She demonstrates growth deficiency and microcephaly with her weight of 12.8 kg (25–50th centile), height of 87.7 cm

(10th centile) and OFC of 44 cm (<3rd centile). Dysmorphic features include hypertelorism, low-set ears and micrognathia.

Patient 5

A 6-year-old girl was born at 38 weeks of gestation, with birth weight of 1870 g (<3rd centile), length of 42 cm (<3rd centile) and OFC of 28 cm (<3rd centile), indicating intrauterine growth restriction. Since early infancy, she exhibited severe hypotonia, and her psychomotor development was severely delayed. She experienced refractory seizures after 1 year of age. Although hydronephrosis was noted by abdominal ultrasonography, there was no abnormal renal function. The brain MRI examined at an age of 4 months revealed a hypoplastic brain associated with complete agenesis of the corpus callosum (Figures 3m–o). As a result of recurrent aspiration pneumonia, laryngotracheal separation surgery was performed. At present, her height is 99 cm (<3rd centile), weight is 15.3 kg (<3rd centile) and OFC of 42 cm (<3rd centile), indicating severe growth deficiency and microcephaly. She can stand by support, but no meaningful words.

Patient 6

A 10-year-old girl was born at 40 weeks and 3 days of gestation. At the age of 3 years, she was referred to our institution because of intractable epilepsy. At that time, neurological examination revealed generalized hypotonia. EEG showed frequent spikes on the left hemisphere. The brain MRI indicated a hypoplastic brain associated with ACC and delayed myelination (Figures 3p–r). Echocardiography revealed mild aortic regurgitation. At present, her height is 115 cm (<3rd centile), weight is 16.3 kg (<3rd centile) and OFC of 48 cm (<3rd centile), indicating growth delay and microcephaly. She shows severe psychomotor developmental delay with sitting by support and no meaningful word.

DISCUSSION

The characteristics of 1q44 deletions have been recognized as growth deficiency, psychomotor developmental delay, epilepsy, microcephaly, brain malformations including ACC, and distinct facial features.[4,6,7,9,11,18] After chromosomal microarray testing has been available for the identification of submicroscopic chromosomal aberrations, many patients with submicroscopic deletions of 1q44 have been identified.[8,10,12,14,15] Now, precise genotype–phenotype correlation has been evaluated through the accumulation of patients with variable deletion sizes, and a minimal essential region has been proposed for expressing the main characteristics of 1q44 deletion syndrome.[7,8,14–16] Ballif *et al.*[17] evaluated 22 patients with small interstitial deletions of 1q44 and demonstrated critical regions for microcephaly, ACC and seizures. Consequently, *AKT3* was reported to be the gene responsible for microcephaly; zinc finger protein 238 gene (*ZNF238*) for ACC; and heterogeneous nuclear ribonucleoprotein U gene (*HNRNPU*) for seizures[17] (Figure 5).

In this study, we identified six patients with the deletions including 1q44. Clinical and genetic findings were summarized in Table 1 and Figure 5, respectively. The presenting patient 1 and 2 showed typical interstitial deletions of 1q44, in which *AKT3* and *ZNF238* are included, and manifested the typical features of mental retardation, microcephaly, ACC and seizures. This evidence supports the findings reported by Ballif *et al.* that the essential features of 1q44 deletion syndrome are derived from deletions of the minimal region including *AKT3* and *ZNF238*.[17] In comparison with these two patients, the other four patients displayed terminal deletion of 1q44 that include the minimal region including *AKT3* and *ZNF238*. Although the chromosomal breakpoint of patient 5 was just on *AKT3*, phenotypic feature of this patient are extremely severe as compared with those of patient 1 and 2 who had interstitial deletion of 1q44. Although Roos *et al.*[18] reported that 1.6 Mb terminal region does not have clinical relevance, because it appears to primarily contain many of the olfactory receptors genes, many genes of unknown functions are included in this 2.6 Mb region (chr1:245 000 000–247 600 000). Thus, this additionally deleted region in patient 5 may also have been responsible for his severe neurological manifestations.

Patient 4 had an additional chromosomal aberration, with a partial trisomy of 5p derived from an unbalanced translocation. However, the phenotypic severity of patient 4 was not significantly different from that of the other patients with 1q43 deletions. Thus, the partial trisomy of 5p identified in patient 4 did not demonstrate an important contribution to the patient's manifestations. Patient 3 showed extremely severe developmental delay, which may have been modified by the hypoglycemia and subsequent intraventricular hemorrhage suffered during the early infantile period.

The deletion regions of the remaining three patients (patient 3, 4 and 6) expanded toward the centromere beyond the critical region for 1q44 deletion syndrome, and several more genes are included in the deletion region in these three patients. Severe volume loss of the brain was revealed in the brain MRI of these three patients, similar to patient 5, and delayed myelination was also seen on the brain MRI of patient 3 and 4 (Figures 3i, l). Although patient 5 exhibited high T2 signal intensities in the white matter, this image was obtained when he was 4 months of age, and we cannot ascertain if this finding indicated delayed myelination. Similarly, because the brain MRI of patient 1, 2 and 6 were obtained after 3 years of age, we cannot determine whether these three patients experienced delayed myelinations in their early infancy. However, delayed myelination, as a finding associated with 1q44 deletion, has not yet been reported in the literature.[17] It may therefore be that the characteristic findings of the patients with expanded deletion beyond the 1q43 region may have clinical implications for delayed myelination. Although many UCSC genes are present in these additional regions, some of these genes may have clinical relevance for delayed myelination observed in patient 3 and 4. The centrosomal protein 170 kDa gene (*CEP170*) is a potential candidate because of its high expression level in the fetal brain.

In this genotype–phenotype correlation study for patients with 1q44 deletions, we revealed that telemetric region beyond the physical position of chr1:245 000 000 may be responsible for severe volume loss of the brain, and the proximal region beyond *AKT3* may be responsible for delayed myelination. The neighboring genes surrounding 1q43q44 may have some modifier effects to the severe brain impairments associated with delayed myelination. To identify them, much more information regarding genotype–phenotype correlations will need to be accumulated for patients with terminal deletion of 1q.

CONFLICT OF INTEREST

The authors declare no conflict of interest.

ACKNOWLEDGEMENTS

We thank the patients and their parents for their gracious participation and support. This work was supported by Grant-in-Aid for Research Activity Start-up for KS and Grant-in-Aid for Scientific Research (C) for TY from the Japan Ministry of Education, Science, Sports and Culture.

1 Knight, S. J., Regan, R., Nicod, A., Horsley, S. W., Kearney, L., Homfray, T. *et al.* Subtle chromosomal rearrangements in children with unexplained mental retardation. *Lancet* **354,** 1676–1681 (1999).
2 Shimojima, K., Sugiura, C., Takahashi, H., Ikegami, M., Takahashi, Y., Ohno, K. *et al.* Genomic copy number variations at 17p13.3 and epileptogenesis. *Epilepsy Res.* **89,** 303–309 (2010).
3 Cardoso, C., Leventer, R. J., Ward, H. L., Toyo-Oka, K., Chung, J., Gross, A. *et al.* Refinement of a 400-kb critical region allows genotypic differentiation between isolated lissencephaly, Miller-Dieker syndrome, and other phenotypes secondary to deletions of 17p13.3. *Am. J. Hum. Genet.* **72,** 918–930 (2003).
4 Gentile, M., Di Carlo, A., Volpe, P., Pansini, A., Nanna, P., Valenzano, M. C. *et al.* FISH and cytogenetic characterization of a terminal chromosome 1q deletion: clinical case report and phenotypic implications. *Am. J. Med. Genet. A* **117A,** 251–254 (2003).
5 Puthuran, M. J., Rowland-Hill, C. A., Simpson, J., Pairaudeau, P. W., Mabbott, J. L., Morris, S. M. *et al.* Chromosome 1q42 deletion and agenesis of the corpus callosum. *Am. J. Med. Genet. A* **138,** 68–69 (2005).
6 van Bever, Y., Rooms, L., Laridon, A., Reyniers, E., van Luijk, R., Scheers, S. *et al.* Clinical report of a pure subtelomeric 1qter deletion in a boy with mental retardation and multiple anomalies adds further evidence for a specific phenotype. *Am. J. Med. Genet. A* **135,** 91–95 (2005).
7 Boland, E., Clayton-Smith, J., Woo, V. G., McKee, S., Manson, F. D., Medne, L. *et al.* Mapping of deletion and translocation breakpoints in 1q44 implicates the serine/threonine kinase AKT3 in postnatal microcephaly and agenesis of the corpus callosum. *Am. J. Hum. Genet.* **81,** 292–303 (2007).
8 Hill, A. D., Chang, B. S., Hill, R. S., Garraway, L. A., Bodell, A., Sellers, W. R. *et al.* A 2-Mb critical region implicated in the microcephaly associated with terminal 1q deletion syndrome. *Am. J. Med. Genet. A* **143A,** 1692–1698 (2007).
9 Merritt, II J. L., Zou, Y., Jalal, S. M. & Michels, V. V. Delineation of the cryptic 1qter deletion phenotype. *Am. J. Med. Genet. A* **143,** 599–603 (2007).
10 Andrieux, J., Cuvellier, J. C., Duban-Bedu, B., Joriot-Chekaf, S., Dieux-Coeslier, A., Manouvrier-Hanu, S. *et al.* A 6.9 Mb 1qter deletion/4.4 Mb 18pter duplication in a boy with extreme microcephaly with simplified gyral pattern, vermis hypoplasia and corpus callosum agenesis. *Eur. J. Med. Genet.* **51,** 87–91 (2008).
11 Hiraki, Y., Okamoto, N., Ida, T., Nakata, Y., Kamada, M., Kanemura, Y. *et al.* Two new cases of pure 1q terminal deletion presenting with brain malformations. *Am. J. Med. Genet. A* **146A,** 1241–1247 (2008).
12 Poot, M., Kroes, H. Y. & Hochstenbach, R. AKT3 as a candidate gene for corpus callosum anomalies in patients with 1q44 deletions. *Eur. J. Med. Genet.* **51,** 689–690 (2008).
13 van Bon, B. W., Koolen, D. A., Borgatti, R., Magee, A., Garcia-Minaur, S., Rooms, L. *et al.* Clinical and molecular characteristics of 1qter microdeletion syndrome: delineating a critical region for corpus callosum agenesis/hypogenesis. *J. Med. Genet.* **45,** 346–354 (2008).
14 Orellana, C., Rosello, M., Monfort, S., Oltra, S., Quiroga, R., Ferrer, I. *et al.* Corpus callosum abnormalities and the controversy about the candidate genes located in 1q44. *Cytogenet. Genome Res.* **127,** 5–8 (2009).
15 Caliebe, A., Kroes, H. Y., van der Smagt, J. J., Martin-Subero, J. I., Tonnies, H., van't Slot, R. *et al.* Four patients with speech delay, seizures and variable corpus callosum thickness sharing a 0.440 Mb deletion in region 1q44 containing the HNRPU gene. *Eur. J. Med. Genet* **53,** 179–185 (2010).
16 Nagamani, S. C., Erez, A., Bay, C., Pettigrew, A., Lalani, S. R., Herman, K. *et al.* Delineation of a deletion region critical for corpus callosal abnormalities in chromosome 1q43-q44. *Eur. J. Hum. Genet.* **20,** 176–179 (2012).
17 Ballif, B. C., Rosenfeld, J. A., Traylor, R., Theisen, A., Bader, P. I., Ladda, R. L. *et al.* High-resolution array CGH defines critical regions and candidate genes for microcephaly, abnormalities of the corpus callosum, and seizure phenotypes in patients with microdeletions of 1q43q44. *Hum. Genet.* **131,** 145–156 (2012).
18 Roos, A., Eggermann, T., Zerres, K. & Schuler, H. M. Polymorphic subtelomeric deletion 1q demonstrates the need to reevaluate subtelomere screening methods: determination of the boundary between pathogenic deletion and benign variant for subtelomere 1q. *Am. J. Med. Genet. A* **146A,** 795–798 (2008).

Supplementary Information accompanies the paper on Journal of Human Genetics website (http://www.nature.com/jhg)

CLINICAL GENETICS An International Journal of Genetics, Molecular and Personalized Medicine

Clin Genet 2013: 83: 135–144
Printed in Singapore. All rights reserved

CLINICAL GENETICS
doi: 10.1111/j.1399-0004.2012.01885.x

Original Article

Exome sequencing in a family with an X-linked lethal malformation syndrome: clinical consequences of hemizygous truncating *OFD1* mutations in male patients

Tsurusaki Y, Kosho T, Hatasaki K, Narumi Y, Wakui K, Fukushima Y, Doi H, Saitsu H, Miyake N, Matsumoto N. Exome sequencing in a family with an X-linked lethal malformation syndrome: clinical consequences of hemizygous truncating *OFD1* mutations in male patients.
Clin Genet 2013: 83: 135–144. © John Wiley & Sons A/S. Published by Blackwell Publishing Ltd, 2012

Oral-facial-digital syndrome type 1 (OFD1; OMIM #311200) is an X-linked dominant disorder, caused by heterozygous mutations in the *OFD1* gene and characterized by facial anomalies, abnormalities in oral tissues, digits, brain, and kidney; and male lethality in the first or second trimester pregnancy. We encountered a family with three affected male neonates having an 'unclassified' X-linked lethal congenital malformation syndrome. Exome sequencing of entire transcripts of the whole X chromosome has identified a novel splicing mutation (c.2388+1G > C) in intron 17 of *OFD1*, resulting in a premature stop codon at amino acid position 796. The affected males manifested severe multisystem complications in addition to the cardinal features of OFD1 and the carrier female showed only subtle features of OFD1. The present patients and the previously reported male patients from four families (clinical OFD1; Simpson-Golabi-Behmel syndrome, type 2 with an *OFD1* mutation; Joubert syndrome-10 with *OFD1* mutations) would belong to a single syndrome spectrum caused by truncating OFD1 mutations, presenting with craniofacial features (macrocephaly, depressed or broad nasal bridge, and lip abnormalities), postaxial polydactyly, respiratory insufficiency with recurrent respiratory tract infections in survivors, severe mental or developmental retardation, and brain malformations (hypoplasia or agenesis of corpus callosum and/or cerebellar vermis and posterior fossa abnormalities).

Conflict of interest

The authors have no conflict of interest to declare.

Y Tsurusaki[a*], T Kosho[b*], K Hatasaki[c], Y Narumi[b], K Wakui[b], Y Fukushima[b], H Doi[a], H Saitsu[a], N Miyake[a] and N Matsumoto[a]

[a]Department of Human Genetics, Yokohama City Graduate School of Medicine, Yokohama, Japan, [b]Department of Medical Genetics, Shinshu University School of Medicine, Matsumoto, Japan, and [c]Department of Pediatrics, Toyama Prefectural Central Hospital, Toyama, Japan

*These authors contributed equally to this work.

Key words: exome sequencing – OFD1 – *OFD1* gene – splicing mutation – X-linked congenital malformation syndrome

Corresponding authors: Tomoki Kosho, MD, Department of Medical Genetics, Shinshu University School of Medicine, 3-1-1 Asahi, Matsumoto, Nagano 390-8621, Japan.
Tel.: +81 263 37 2618;
fax: +81 263 37 2619;
e-mail: ktomoki@shinshu-u.ac.jp
and
Naomichi Matsumoto, MD, PhD, Department of Human Genetics, Yokohama City Graduate School of Medicine, 3-9 Fukuura, Kanazawa-ku, Yokohama 236-0004, Japan.
Tel.: +81 45 787 260;
fax: +81 45 786 5219;
e-mail: naomat@yokohama-cu.ac.jp

Received 14 January 2012, revised and accepted for publication 26 March 2012

Oral-facial-digital syndrome type 1 (OFD1; OMIM #311200), originally described by Papillon-Leage and Psaume (1) and further delineated by Gorlin and Psaume (2), is an X-linked dominant developmental disorder with an estimated prevalence of 1:50,000, caused by mutations in the *OFD1* gene (OMIM #300170) (3–5). The disorder is characterized by facial anomalies and abnormalities in oral tissues, digits, brain and kidney (5). Almost all affected individuals with OFD1 are female, with highly variable expression, possibly resulting from random X inactivation (6). Affected males are generally lost in the first or second trimester of pregnancy (4). To date, only one liveborn male case with clinically definite OFD1 and a normal karyotype has been reported; the patient was born at 34 weeks of gestation and died 21 h after birth due to heart failure (7). In this report, we describe a family with three affected male neonates having an 'unclassified' X-linked lethal congenital malformation syndrome. Exome sequencing of entire transcripts of the whole X chromosome has successfully identified a causative splicing mutation in *OFD1*.

Subjects and methods

Clinical report

II-2, a 22-year-old woman, was referred to our clinic for genetic counseling (Fig. 1). Her deceased brother (II-4) had severe multiple congenital abnormalities. She had two sons (III-1 and III-5) with similar congenital abnormalities and a healthy boy (III-3) as well as two miscarriages (III-2, artificial; III-4, spontaneous). During genetic counseling and molecular investigations, she had another healthy boy (III-5). After identification of a heterozygous *OFD1* mutation, she was examined for features of OFD1. Only a few accessory frenulae and irregular teeth with no facial anomalies or tongue abnormalities were observed (Fig. 2a–e). A radiograph of her hands showed no abnormalities (Fig. 2f) and an abdominal ultrasonography detected no cysts in the kidneys, liver, or pancreas (data not shown). I-2, allegedly, had no apparent malformations or complications including renal diseases.

II-4 was born by caesarean section because of placental abruption at 33 weeks of gestation. Pregnancy was complicated by polyhydramnios. Apgar score was 3 at 1 min. His birth weight was 2056 g (+0 SD), length was 45.0 cm (+0.5 SD), and occipitofrontal circumference (OFC) was 34.0 cm (+2.0 SD). He manifested severe respiratory insufficiency and was transferred to a neonatal intensive care unit (NICU). His craniofacial features included a prominent forehead, a large fontanelle (5 × 5 cm), a low posterior hairline, microphthalmia, hypertelorism, short palpebral fissures, depressed nasal bridge, low-set ears, a small cleft lip and a soft cleft palate, narrowing of the tip of the tongue, and a hypoplastic gum (Fig. 2g). Additional physical features included redundant neck skin, postaxial polydactyly of the left hand (Fig. 2h), wide halluces (Fig. 2i), micropenis, and left cryptorchidism.

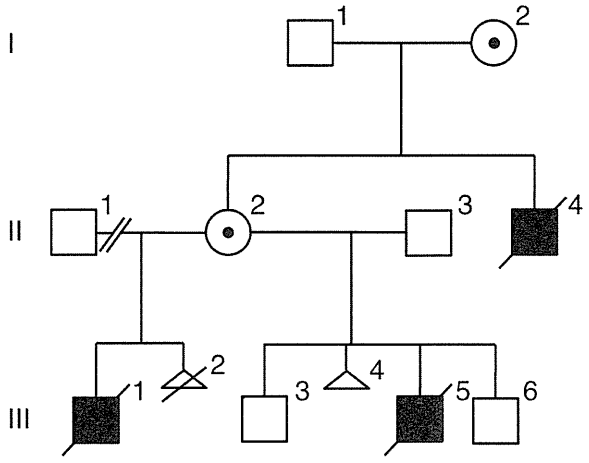

Fig. 1. Familial pedigree.

Ultrasonography revealed hypoplastic gyri, an atrial septal defect, and patent ductus arteriosus. Ophthalmological examination detected microcornea and retinal detachment. Intubation was impossible because of laryngeal anomalies and the patient died 11 h after birth. Additional autopsy findings included partial atelectasis and bilateral hydroureters.

III-1 was delivered by emergency caesarean section at 39 weeks of gestation. Pregnancy was complicated by polyhydramnios and intrauterine growth retardation, with moderate macrocephaly. His birth weight was 3064 g (+0.1 SD). He was admitted to a NICU because of respiratory insufficiency, and received mechanical ventilation. His craniofacial features included microphthalmia, hypertelorism, short palpebral fissures, epicanthus, low-set ears, and a cleft lip and palate. Additional physical features included bilateral polydactyly of hands (postaxial) and feet (preaxial), and an ectopic urethral opening. Ultrasonography revealed hydrocephalus, agenesis of the corpus callosum and cerebellar vermis, and a complete atrioventricular septal defect. Ophthalmological examination detected persistent pupillary membrane and optic disc coloboma. G-banded chromosomes were normal (46,XY). The patient died at age 14 days due to heart failure.

III-5 was delivered by caesarean section at 32 weeks of gestation. Pregnancy was complicated by polyhydramnios, intrauterine growth retardation, and congenital heart defects. His birth weight was 1704 g (−0.2 SD), length was 40.0 cm (−0.8 SD), and OFC was 33.3 cm (+2.0 SD). He was admitted to a NICU because of respiratory insufficiency, and received mechanical ventilation. His craniofacial features included a prominent forehead, hypertelorism, dysplastic ears, a small cleft lip, and a soft cleft palate (Fig. 2j,k). Ultrasonography revealed hydrocephalus with Dandy-Walker malformation and hypoplastic left heart syndrome. G-banded chromosomes were normal (46,XY). The patient died 1 day after birth. Additional autopsy findings included agenesis of the cerebellar vermis (Fig. 2l), enlargement of the fourth ventricle and aqueduct, anomalous positioning of the esophagus, mild

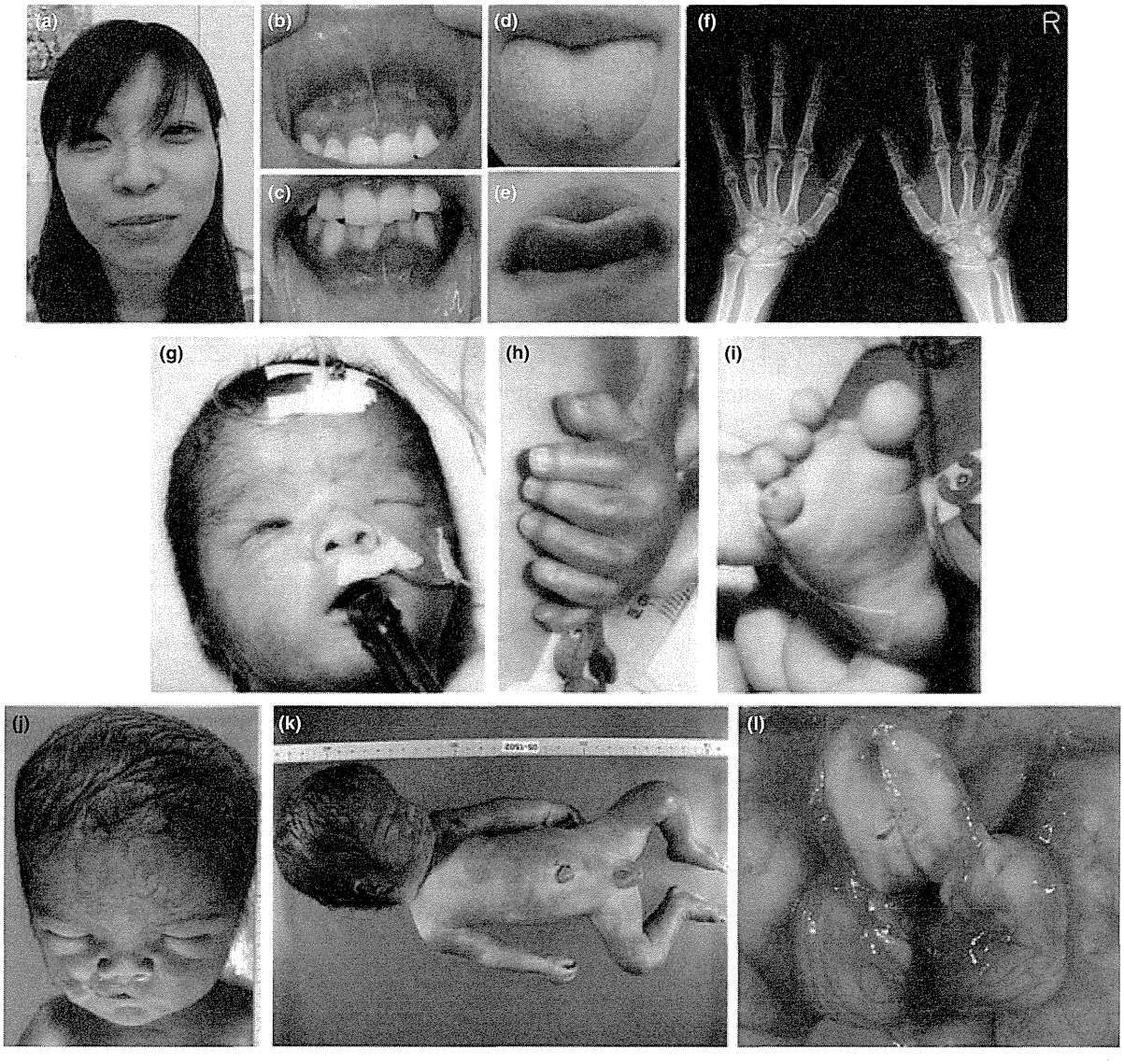

Fig. 2. Clinical photographs of II-2 (**a–f**), II-4 (**g–i**), and III-5 (**j–l**).

pulmonary congestion, and insufficient lobulation of the right lung.

The three affected male neonates, having strikingly similar clinical manifestations (Table 1), are considered to have had a congenital malformation syndrome with X-linked inheritance. Array-CGH analysis using 4200 BAC clones identified no pathologic genomic copy number abnormalities. Direct sequencing of *MID*, performed because of a partial similarity to these neonates' syndrome to X-linked Opitz-G/BBB syndrome (OMIM #300000) (8), revealed no mutation.

Library preparation

Genomic DNA for II-2, II-3, III-3, and III-6 was extracted from peripheral blood using the Gentra PureGene Blood Kit (QIAGEN, Hilden, Germany), and genomic DNA for III-5 was extracted from the preserved dried umbilical cord using the DNeasy Blood & Tissue Kit (QIAGEN). Three micrograms of high-quality (absorbance at 260 nm/absorbance at 280 nm: 1.8–2.0) genomic DNA from II-2 was fragmented using the Covaris model S2 system (Covaris, Woburn, MA). The target peak size was 150 bp. After the size of sheared DNA was checked using an Agilent 2100 Bioanalyzer (Agilent Technologies, Santa Clara, CA), adapter sequences were ligated to the ends of DNA fragments, and amplified according to the manufacturer's protocol (Agilent Technologies).

Exome capture and next-generation sequencing

Library DNA was hybridized for 24 h at 65°C using the SureSelect Human X Chromosome Demo Kit (Agilent Technologies). Captured DNA was diluted to a concentration of 8 pM and sequenced on a Genome Analyzer IIx (Illumina, San Diego, CA) with 76-bp paired-end reads. We used only one of the eight lanes in the flow

Table 1. Variant priority scheme after exome sequencing[a]

	NextGENe	II-2	MAQ (SeattleSeq)
Total variants called	22,176	—	58,081
Chr X	3441	—	4383
Unknown SNP variants	910	—	882
(dbSNP131, 1000 genomes)	—	—	—
Overlap of NextGENe and MAQ	—	169	—
NS/SS	—	17	—
Except for variants at segmental duplications	—	15	—

NS, non-synonymous; SNP, single-nucleotide polymorphism; SS, splice site (±2).
[a]MAQ was annotated with SeattleSeq Annotation. The annotation includes gene names, dbSNP rs ID, and SNP functions (e.g. missense), protein positions and amino acid changes.

cell for II-2 (Illumina). Image analyses and base calling were performed using sequence control software real-time analysis and Offline Basecaller software v1.8.0 (Illumina). Reads were aligned to the human reference genome (UCSC hg19, NCBI build 37.1).

Mapping strategy and variant annotation

The quality-controlled (Path Filter) reads were mapped to the human reference genome (UCSC hg19, NCBI build 37.1), using mapping and assembly with quality (MAQ) and NextGENe software v2.0 (SoftGenetics, State College, PA). Single-nucleotide polymorphisms in MAQ-passed reads were annotated using the SeattleSeq Annotation website (http://gvs.gs.washington.edu/SeattleSeqAnnotation/).

Priority scheme and capillary sequencing

Called variants found by each informatics method were filtered in terms of location on chromosome X, unregistered variants (excluding registered dbSNP131 and 1000 Genomes), overlapping variants called in common by NextGENe and MAQ, and non-synonymous changes and splice-site mutations (±2 bp from exon–intron junctions) (Table 1). The variants were confirmed as true positives by Sanger sequencing of polymerase chain reaction (PCR) products amplified using genomic DNA as a template, except for variants within genes at segmental duplications. Sanger sequencing was performed on an ABI3500xl or ABI3100 autosequencer (Life Technologies, Carlsbad, CA). Sequencing data were analyzed using Sequencher software (Gene Codes Corporation, Ann Arbor, MI).

Reverse transcription-PCR

Total RNA was isolated from EBV-transformed lymphoblastoid cell line (EBV-LCL) derived from II-2 and healthy control subjects using the RNeasy Plus Mini Kit (QIAGEN). Five micrograms of total cellular RNA was used for reverse transcription with the Super Script III First-Strand Synthesis System (Life Technologies). Two microliters of synthesized complementary DNA was used for PCR with the following primers: ex17-F (5′-CTACCATCACCCACTGAGTC-3′) and ex19-R (5′-TGAGACATATCCCCGGCAG-3′). Amplified PCR products were electrophoresed in agarose gels, purified from gels using the QIAquick Gel Extraction Kit (QIAGEN), cloned into pCR4-TOPO vector (Life Technologies) and sequenced.

X-chromosome inactivation assay

The human androgen receptor (HUMARA) assay was performed as previously reported (9). Genomic DNA of II-2 was digested at 37°C for 18 h with two methylation-sensitive enzymes, *Hpa*II and *Hha*I. PCR was performed using digested and undigested DNA with HUMARA primers (FAM-labeled ARf: 5′-TCCAGAATCTGTTCCAGAGCGTGC-3′; ARr: 5′-CTCTACGATGGGCTTGGGGAGAAC-3′). DNA fragment analysis was performed on an ABI3130xl autosequencer (Life Technologies). Fragment data were analyzed with GeneMappert Software version 4.1 (Life Technologies).

Results

Exome sequencing

Because this disorder was assumed to be an 'X-linked recessive' disorder based on the initial pedigree information, we focused on the X chromosome. Approximately 4.5 Gb of sequence data were generated, 87.3% of which was mapped to the human reference genome (UCSC hg19, NCBI build 37.1). MAQ was able to align 53,242,972 reads to the whole genome.

Two informatics methods identified 17 potential pathogenic changes (15 missense mutations, 1 nonsense mutation, and 1 splice-site mutation) (Table 1). The nonsense mutation was a false positive and all 13 missense mutations were inconsistent with the phenotype (no co-segregation). The mutation c.2388+1G>C was identified at the splice-acceptor site of intron 17 in *OFD1*, heterozygously in II-2, and hemizygously in III-5, but was absent in II-3, III-3, and III-6 (Fig. 3a) as well as 93 normal female controls (0/186 alleles).

RT-PCR, direct sequencing

To examine the mutational effects of c.2388+1G>C, reverse transcriptase-polymerase chain reaction (RT-PCR) was performed. Only a 239-bp PCR product (wild-type allele) was observed in healthy control individuals (Fig. 3b). By contrast, a longer 1364-bp product was detected in II-2. Sequencing of the 1364-bp product revealed that a 1125-bp sequence of intron 17 was retained, producing a premature stop codon at amino acid position 796 (Fig. 3b). These data indicate

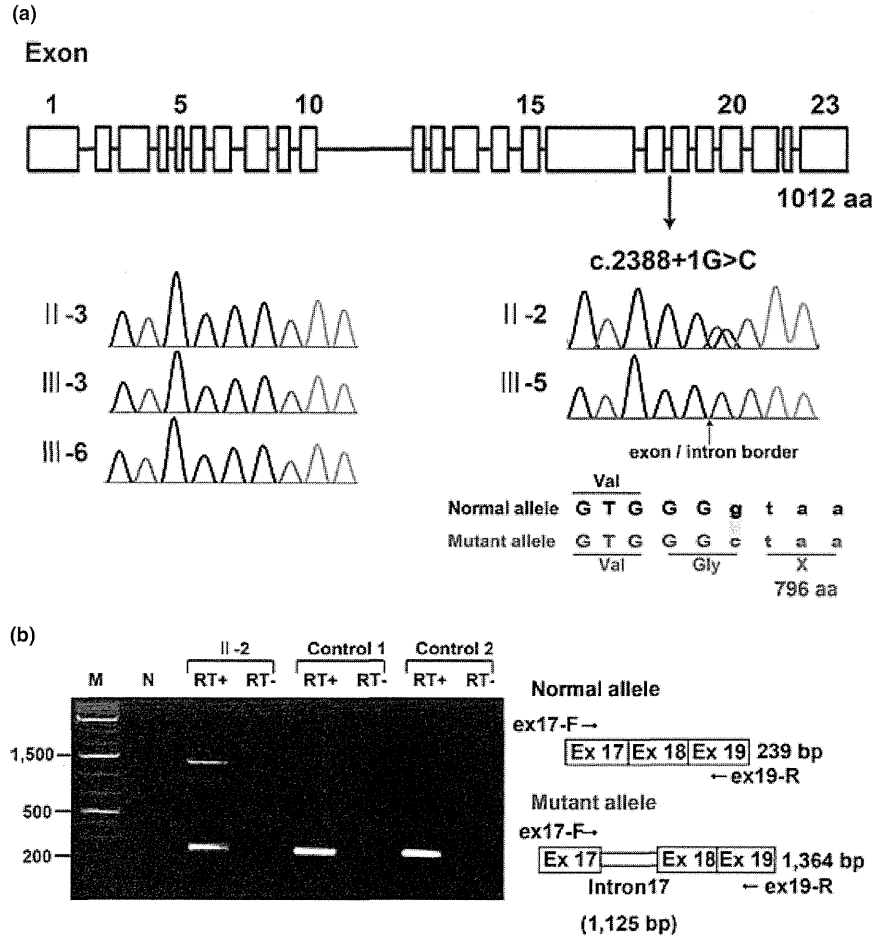

Fig. 3. (**a**) Gene structure of *OFD1* with the mutation (c.2388+1G>C) (upper). Electropherograms of the family members. Wild-type sequences are seen in II-3, III-3 and III-6. Heterozygous and hemizygous mutations are observed in II-2 and III-5, respectively. (**b**) Reverse transcriptase-polymerase chain reaction analysis showing both 239-bp and 1364-bp products in II-2, and only 239-bp products in two normal female controls. The 239-bp product is normal and the 1364-bp product is aberrant.

that the c.2388+1G>C mutation in *OFD1* is most likely the causal mutation in this family.

X-chromosome inactivation assay

X-chromosome inactivation patterns was random patterns in II-2 available for this study (ratio > 38:62).

Discussion

Exome sequencing detected a single-base substitution (c.2388+1G>C) in *OFD1*, resulting in an error in splicing of intron 17 and a premature stop codon at amino acid position 796, in an affected male (III-5) and a carrier female (II-2) in this family with an 'unclassified' X-linked lethal congenital malformation syndrome. II-4 and III-1, who had strikingly similar clinical manifestations to III-5, are likely to have had the same *OFD1* mutation as III-5, although their DNA was not available. Through reassessment of clinical features of the family, the three affected males shared facial, oral, and digital malformations characteristic of OFD1 (4). Additionally, they exhibited more severe complications in various systems including congenital heart defects, genitourinary malformations, and ophthalmological abnormalities. II-2 was also found to have subtle features of OFD1 (accessory frenulae and irregular teeth). Thus, we have concluded that the 'unclassified' X-linked lethal congenital malformation syndrome in this family was clinically compatible with OFD1.

An *OFD1* mutation (c.2123_2126dupAAGA in exon 16, p.Asn711Lysfs*3) was also detected in a family with an X-linked recessive mental retardation syndrome (10). Nine affected males had macrocephaly and severe mental or developmental retardation, and suffered from recurrent respiratory tract infections leading to early death in eight. Only an 11-year-old boy survived with severe mental retardation (IQ 20), obesity, and brachydactyly. His younger brother had postaxial polydactyly. No cognitive, oral, facial, digital, or renal abnormalities were detected in heterozygous carrier females in that family. The patients were later classified into an infantile lethal variant of Simpson-Golabi-Behmel syndrome (type 2) (SGBS2, OMIM #300209), which had consisted of only one family,

genetically mapped to Xp22, including four maternally related affected males with hydrops at birth, craniofacial anomalies (macrocephaly, low-set posteriorly angulated ears, hypertelorism, short and broad nose with anteverted nares, large mouth with thin upper vermilion border, prominent philtrum, high-arched or cleft palate, and short neck), redundant skin, hypoplastic nails, skeletal defects involving upper and lower limbs, gastrointestinal and genitourinary anomalies, hypotonia and neurological impairment, and early death within the first 8 weeks (11, 12). Other *OFD1* mutations were detected in two families with Joubert syndrome-10 (JBTS10, OMIM #213300) (13). A mutation (c.2844_2850delAGACAAA in exon 21, p.Lys948Asnfs*9) in a family with eight affected males caused severe mental or developmental retardation and recurrent infections in all; postaxial polydactyly in five, retinitis pigmentosa in three, and a molar tooth sign on brain magnetic resonance imaging (MRI) in two. No heterozygous carrier females had any symptoms similar to those in the affected males. Another mutation (c.2767delG in exon 21, p.Glu923Lysfs*4) was found *de novo* in a 12-year-old male patient with severe mental retardation, macrocephaly, obesity, postaxial polydactyly, and a molar tooth sign on brain MRI (13).

To discuss whether these male patients with hemizygous truncating *OFD1* mutations would have different conditions (OFD1, SGBS2, or JBTS10) or belong to the same syndrome spectrum, we have created a comprehensive list of clinical manifestations in all of them (Table 2) (7, 10, 13). Macrocephaly, polydactyly (postaxial), respiratory insufficiency with recurrent respiratory tract infections in survivors, and severe mental or developmental retardation were shared by all the families (7, 10, 13). Nasal bridge features (depressed or broad) and lip abnormalities (cleft lip, pseudocleft lip, full lips, and prominent philtrum) were shared by the families with OFD1 and JBTS10 (7, 13). Brain malformations including hypoplasia or agenesis of corpus callosum, hypoplasia or agenesis cerebellar vermis as well as posterior fossa abnormalities (large, occipital encephalocele) were also shared by the families with OFD1 and JBTS10 (7, 13). III-5 in the present family was described to have Dandy-Walker malformation on brain ultrasonography. Three patients with JBTS10 were described to have a molar tooth sign on brain MRI, which is the characteristic neuroradiological hallmark of Joubert syndrome (13). Dandy-Walker malformation, typically consisting of agenesis or hypoplasia of cerebellar vermis, a cystic dilatation of the fourth ventricle, and an enlarged posterior fossa with a high position of the tentorium, is usually distinguishable from Joubert syndrome, characterized anatomically by agenesis or hypoplasia of cerebellar vermis and enlargement of the superior cerebellar peduncles and deep interpeduncular fossa resulting from a lack of normal decussation of superior cerebellar peduncular fiber tracts, leading to the characteristic 'molar tooth' appearance on transverse computed tomography and MRI of the midbrain (14); and clinically by hypotonia, developmental retardation, abnormal respiratory patterns, and oculomotor apraxia (15). However, Joubert syndrome could be present in association with Dandy-Walker malformation (15); and in such a case, Dandy-Walker malformation was reported to have initially masked the molar tooth sign because of a cystic dilatation of the fourth ventricle (16). Some authors state that the presence of the molar tooth sign does not, in itself, allow a diagnosis, Joubert syndrome, to be made; but that clinical evidence of the syndrome including hypotonia and developmental retardation accompanied by either abnormal breathing or abnormal eye movements should be present (14, 17). Typical respiratory abnormalities in Joubert syndrome, represented by short alternate episodes of apnea and hyperpnea or episodic hyperpnea alone (18), were not described in the patients with JBTS10, with only one presenting with stridor and intermittent cyanosis soon after birth (13). Abnormal eye movements including oculomotor apraxia were not mentioned in those with JBTS10 (13). In view of these evidences, it is reasonable to consider that the male patients with *OFD1* mutations, identified to date, would belong to a clinical continuum with wide intra- and inter-familial phenotypic variations of a single disorder.

A review by Macca and Franco (4) summarized all reported mutations in OFD1 patients. In total, 99 different mutations (7 genomic deletions and 92 point mutations) were identified, including 67 frameshift mutations (58%), 14 missense mutations (12%), 14 splice-site mutations (12%), 13 nonsense mutations (11%), and an in-frame deletion. Point mutations occur only in the first 17 exons (*OFD1* consists of 23 exons). A significant genotype–phenotype correlation between high-arched/cleft palate and missense and splice-site mutations has been identified (19). In addition, cystic kidney is more frequently associated with mutations in exons 9 and 12 (19). Quantitative PCR analysis of *OFD1* mRNA levels in EBV-LCLs from two families with JBTS10 showed that 30% and 58% of *OFD1* expression remained, suggesting that the mutant mRNA would be subject to nonsense-mediated decay and that the phenotypic variability observed for *OFD1* mutations would be caused by changes in activity of remaining truncated OFD1 protein (13). To date, premature stop codons at 713 in exon 16 (19), 796 in exon 17 (this report), 926 in exon 21 (13), and 956 in exon 21 (13) are associated with survival in males with hemizygous truncating *OFD1* mutations and no or subtle clinical manifestations in females with heterozygous *OFD1* mutations. Heterozygous truncating *OFD1* mutations preserving normal exons 1–16 have been reported in only two families with typical female OFD1 patients: a single-base deletion (c.2349delC in exon 17, p.Ileu784Serfs*85) (20) and a deletion of complete exon 17 (21). Mutations producing longer truncated protein (~ exon 17) might cause a milder form of the disorder that could not be detected in typical female OFD1 patients, but could be detected in male patients with multiple congenital anomalies and probable lethality in childhood.

Table 2. Clinical features of male patients with *OFD1* mutations

	Family 1 (present family)			Family 2[b]	Family 3[c]				Family 4[d] (W07-713)			Family 5[d]	Carrier
Patient	II-4	III-1	III-5	1	IV-1	IV-3	IV-11	6 Patients	III-9	IV-10	6 Patients	(UW87)	19 Females
Age	0d/D	14d/D	1d/D		11 y	18 m/D	3 y/D	D	34 y	3.5 y	D (3)		
Birth weight (g) (gestational age)	2056 (33)	3064 (39)	1704 (32)		3850 (40)	4120 (38)	1915 (35)			3050 (Te)		4090 (41)	
Macrocephaly (>1.5 SD)	+		+		+	+	+	Some				+	
Obesity					+				−	−	−	+	
Craniofacial (87.3%[a])									−	−	−		
Facial anomalies (69.1%[a])													
Prominent forehead	+		+										
Redundant neck skin	+											+	
Hypertelorism	+	+	+	+									
Epicanthus		+											
Short palpebral fissures	+	+											
Nasal bridge features	Dep		Dep						Br	Br		Dep	
Low-set ears	+	+			+				+	+			
Lip abnormalities (32.6%[a])	PCL	CL	PCL	PCL					F_L, PP	F_L, PP		PCL	PCL (1)
Oral													
Palatal abnormalities (49.6%[a])	CSP	CP	CSP	CSP	HP								
Accessory frenulae (63.7%[a])													+ (4)
Tongue abnormalities (84.1%[a])	Nar											MG	Lob (3)
Teeth abnormalities (43.3%[a])													Ir (1)
Skeletal													
Short fingers/brachydactyly					+		+			−		+	
Postaxial polydactyly (3.7%[a])	LtH	BiH		BiHRtBLT		RtH			−	BiHF	BiHF (4)	BiHLtF	
Preaxial polydactyly (19.3%[a])	BiBrHx	BiF		BiBHx	BiBrT								
Respiratory													
Laryngeal anomalies	+												
Respiratory insufficiency	+	+				+				+			
Recurrent infections					+	+	+	+	+	+	+ (6)	+	
Cardiovascular													
Congenital heart defects	ASD, PDA	AVSD	HLHS	AVSD						−			
Genitourinary													
Cystic kidney	−		−		−	−			−	−	−	−	
Urinary tract abnormalities	HU	EUO											
Genital abnormalities	MP, C												
Gastrointestinal													
Esophageal abnormalities			+										
Ophthalmological													
Microphthalmia/microcornea	+												
Persistent papillary membrane		+											

Table 2. Continued

Patient	Family 1 (present family)			Family 2[b]	Family 3[c]				Family 4[d] (W07-713)			Family 5[d]	Carrier
	II-4	III-1	III-5	1	IV-1	IV-3	IV-11	6 Patients	III-9	IV-10	6 Patients	(UW87)	19 Females
Optic disc coloboma		+											
Optic nerve atrophy												+	
Retinal detachment	+												
Retinitis pigmentosa									+	+	+ (1)	−	
Central nervous system (48.4%[a])													
Hydrocephalus		+	+	+	−	−	+						
Gyrus abnormalities	Hp			PM	−	−	−						
Corpus callosum abnormalities		Ag		Ag	−	−	−					Hp	
Cerebellar vermis abnormalities		Ag	Ag		−	−	−		Hp	Hp			
Thick superior cerebellar peduncles					−	−	−		+	+			
Molar tooth sign					−	−	−		+	+		+	
Dandy-Walker malformation			+		−	−	−						
Posterior fossa abnormalities				L	−	−	−			L		EC	
Developmental/mental retardation					S	S	+	S	S	S	+ (All)	S	

+, present; −, absent; blank, data not available; Ag, agenesis; ASD, atrial septal defect; AVSD, atrioventricular septal defect; BHx, bifid halluces; Bi, bilateral; BLT, bifid little toe; Br, broad; C, cryptorchidism; CL, cleft lip; CP, cleft palate; CSP, cleft soft palate; d, days; D, death; Dep, depressed; EC, encephalocele; EUO, ectopic urethral opening; F, foot/feet; FL, full lips; H, hand(s); HF, hands and feet; HLHS, hypoplastic left heart; Hp, hypoplasia; HP, high palate; HU, hydroureter; Hx, halluces; Ir, irregular; L, large; Lob, lobulated; Lt, left; m, months; MG, midline groove; MP, micropenis; Nar, narrowing of the tip of the tongue; PCL, pseudocleft of the upper lip; PDA, patent ductus arteriosus; PM, polymicrogyria; PP, prominent philtrum; Rt, right; S, severe; Te, term; T, thumbs; y, years.

[a]From Macca and Franco (4).

[b]From Goodship et al. (7).

[c]From Budny et al. (10).

[d]From Coene et al. (13).

High-throughput, next-generation sequencing (NGS) has had a tremendous impact on human genetic research (22). Moreover, techniques enabling enrichment of selected regions enable us to use NGS efficiently and to identify the causative genes for a reasonable number of genetic disorders as well as susceptibility genes for complex diseases and health-related traits (23). In particular, X-linked disorders are good candidates for exome sequencing. We recently identified a nonsense mutation in *MCT8* causing X-linked leukoencephalopathy in a family from only two affected male samples (24). We have also identified two possible but inconclusive missense variants (*L1CAM* and *TMEM187*) in a family with an atypical X-linked leukodystrophy from only two affected male samples (25). In this study, exome sequencing accompanied by appropriate bioinformatics techniques and a co-segregation evaluation successfully revealed a disease-causing mutation in *OFD1*, which could not have been assumed to be a candidate based on the clinical manifestations of the affected male patients. Unbiased rapid screening through these technologies is a powerful method for the detection of mutations in unexpected causative genes in undiagnosed patients with multiple congenital malformations.

In conclusion, we have identified a causative splicing mutation in *OFD1*, through exome sequencing, in a family with three males having an 'unclassified' X-linked lethal congenital malformation syndrome. The affected males manifested severe multisystem complications in addition to the cardinal features of OFD1 and the carrier female showed only subtle features of OFD1. The present patients, as well as the previously reported male patients from four families (one with clinical OFD1; one with SGBS2 and an *OFD1* mutation; two with JBTS10 and *OFD1* mutations), would belong to a single syndrome spectrum caused by truncating *OFD1* mutations, presenting with craniofacial features (macrocephaly, depressed or broad nasal bridge, and lip abnormalities), postaxial polydactyly, respiratory insufficiency with recurrent respiratory tract infections in survivors, severe mental or developmental retardation, and brain malformations (hypoplasia or agenesis of corpus callosum and/or cerebellar vermis and posterior fossa abnormalities).

Acknowledgements

The authors are grateful to the family for their participation in this study. The authors are also thankful to Prof Germana Meroni (Cluster in Biomedicine, Trieste) for mutation analysis of *MID1*, Dr Takeshi Futatani (Department of Pediatrics, Toyama Prefectural Central Hospital, Toyama, Japan), Dr Masahiko Kawabata (Department of Internal Medicine, Toyama Prefectural Central Hospital, Toyama, Japan), and Dr Akio Uchiyama (Department of Pathology, Toyama Prefectural Central Hospital, Toyama, Japan) for collecting clinical information; Dr Gen Nishimura (Department of Radiology, Tokyo Metropolitan Children's Medical Center) for helping radiological assessment; and Miss Junko Kunimi (Department of Medical Genetics, Shinshu University School of Medicine, Matsumoto, Japan) and Dr Shin-ya Nishio (Department of Otolaryngology, Shinshu University School of Medicine, Matsumoto, Japan) for their technical assistance. This work was supported by research grants from the Ministry of Health, Labour and Welfare (T. K., Y. F., H. S., N. Mi., and N. Ma.), the Japan Science and Technology Agency (N. Ma.), the Strategic Research Program for Brain Sciences (N. Ma.) and a Grant-in-Aid for Scientific Research on Innovative Areas (Foundation of Synapse and Neurocircuit Pathology) from the Ministry of Education, Culture, Sports, Science and Technology of Japan (N. Ma.), a Grant-in-Aid for Scientific Research from Japan Society for the Promotion of Science (N. Ma.), a Grant-in-Aid for Young Scientist from Japan Society for the Promotion of Science (H. S. and N. Mi.) and a grant from the Takeda Science Foundation (N. Mi. and N. Ma.). This work was performed at the Advanced Medical Research Center, Yokohama City University, Japan.

Y. T., H. D., H. S., and N. Mi. performed the genetic analysis; T. K., K. H., Y. N., K. W., and Y. F. evaluated clinical aspects of the family, recruited samples, and prepared them for the analysis. Y. T., T. K. and N. Ma. wrote the manuscript.

Ethics approval

The work was approved by the Yokohama City University (Faculty of Medicine) and the Shinshu University (School of Medicine). Patient consent was obtained.

References

1. Papillon-Leage M, Psaume J. Une malformation hereditaire de la muquese buccale: brides et freins anomaux. Rev Stomatol 1954: 55: 209–227.
2. Gorlin RJ, Psaume J. Orofaciodigital dysostosis: a new syndrome. A study of 22 cases. J Pediatr 1962: 61: 520–530.
3. Ferrante MI, Giorgio G, Feather SA et al. Identification of the gene for oral-facial-digital type I syndrome. Am J Hum Genet 2001: 68: 569–576.
4. Macca M, Franco B. The molecular basis of oral-facial-digital syndrome, type 1. Am J Med Genet C 2009: 151C: 318–325.
5. Toriello HV, Franco B. Oral-facial-digital syndrome type I. In: Pagon RA, Bind TD, Dolan CR, Stephans K, Adam MP, eds. GeneReviews at genetests: Medical Genetics Information Resource (database online). Seattle, WA: Copyright, University of Washington, 1993–2011, from http://www.genetests.org. Accessed on July 23, 2011.
6. Morleo M, Franco B. Dosage compensation of the mammalian X-chromosome influences the phenotypic variability of X-linked dominant male-lethal disorders. J Med Genet 2008: 45: 401–408.
7. Goodship J, Platt J, Smith R, Burn J. A male with type I orofaciodigital syndrome. J Med Genet 1991: 28: 691–694.
8. Fontanella B, Russolillo G, Meroni G. MID1 mutations in patients with X-linked Opitz G/BBB syndrome. Hum Mutat 2008: 29: 584–594.
9. Nishimura-Tadaki A, Wada T, Bano G et al. Breakpoint determination of X;autosome balanced translocations in four patients with premature ovarian failure. J Hum Genet 2011: 56: 156–160.
10. Budny B, Chen W, Omran H et al. A novel X-linked recessive mental retardation syndrome comprising macrocephaly and ciliary dysfunction is allelic to oral-facial-digital type I syndrome. Hum Genet 2006: 120: 171–178.
11. Terespolsky D, Farrrell SA, Siegel-Bartelt J, Weksberg R. Infantile lethal variant of Simpson-Golabi-Behmel syndrome associated with hydrops fetalis. Am J Med Genet 1995: 59: 329–333.
12. Brzustowicz LM, Farrell S, Khan MB, Weksberg R. Mapping of a new SGBS locus to chromosome Xp22 in a family with a severe form of Simpson-Golabi-Behmel syndrome. Am J Hum Genet 1999: 65: 779–783.
13. Coene KL, Roepman R, Doherty D et al. OFD1 is mutated in X-linked Joubert syndrome and interacts with LCA5-encoded lebercilin. Am J Hum Genet 2009: 85: 465–481.
14. McGraw P. The molar tooth sign. Radiology 2002: 229: 671–672.
15. Chance PF, Cavalier L, Satran D, Pellegrino JE, Koenig M, Dobyns WB. Clinical nosologic and genetic aspects of Joubert and related syndromes. J Child Neurol 1999: 14: 660–666.

16. Sartori S, Ludwig K, Fortuna M et al. Dandy-Walker malformation masking the molar tooth sign: an illustrative case with magnetic resonance imaging follow-up. J Child Neurol 2010: 25: 1419–1422.
17. Barkovich AJ. Anomalies with cerebellar dysgenesis: vermian dysgenesis. In: Barkovich AJ, ed. Pediatric neuroimaging, 4th edn. Lippincott Williams & Wilkins, Philadelphia 2005: 391–396.
18. Brancati F, Dallapiccola B, Valente EM. Joubert syndrome and related disorders. Orphanet J Rare Dis 2010: 5: 20.
19. Prattichizzo C, Macca M, Novelli V et al. Mutational spectrum of the oral-facial-digital type I syndrome: a study on a large collection of patients. Hum Mutat 2008: 29: 1237–1246.
20. Thauvin-Robinet C, Cossée M, Cormier-Daire V et al. Clinical, molecular, and genotype-penotype correlation studies from 25 cases of oral-facial-digital syndrome type 1: a French and Belgian collaborative study. J Med Genet 2006: 43: 54–61.
21. Thauvin-Robinet C, Franco B, Saugier-Veber P et al. Genomic deletions of *OFD1* account for 23% of oral-facial-digital type 1 syndrome after negative DNA sequencing. Hum Mutat 2008: 30: E320–E329.
22. Shendure J, Ji H. Next-generation DNA sequencing. Nat Biotechnol 2008: 26: 1135–1145.
23. Bamshad MJ, Ng SB, Bigham AW et al. Exome sequencing as a tool for Mendelian disease gene discovery. Nat Rev Genet 2011: 12: 745–755.
24. Tsurusaki Y, Osaka H, Hamanoue H et al. Rapid detection of a mutation causing X-linked leukodystrophy by exome sequencing. J Med Genet 2011: 48: 606–609.
25. Tsurusaki Y, Okamoto N, Suzuki Y et al. Exome sequencing of two patients in a family with atypical X-linked leukodystrophy. Clin Genet 2011: 80: 161–166.

RESEARCH ARTICLE

AMERICAN JOURNAL OF medical genetics PART A

Recessive *RYR1* Mutations in a Patient With Severe Congenital Nemaline Myopathy With Ophthalomoplegia Identified Through Massively Parallel Sequencing

Eri Kondo,[1] Takafumi Nishimura,[2] Tomoki Kosho,[3] Yuji Inaba,[2] Satomi Mitsuhashi,[4] Takefumi Ishida,[2] Atsushi Baba,[2] Kenichi Koike,[2] Ichizo Nishino,[4] Ikuya Nonaka,[4] Toru Furukawa,[5] and Kayoko Saito[1]***

[1]Institute of Medical Genetics, Tokyo Women's Medical University, Tokyo, Japan

[2]Department of Pediatrics, Shinshu University School of Medicine, Matsumoto, Japan

[3]Department of Medical Genetics, Shinshu University School of Medicine, Matsumoto, Japan

[4]Department of Neuromuscular Research, National Institute of Neuroscience, National Center of Neurology and Psychiatry, Kodaira, Tokyo, Japan

[5]Tokyo Women's Medical University Institute for Integrated Medical Sciences, Tokyo, Japan

Received 1 October 2011; Accepted 8 January 2012

Nemaline myopathy (NM) is a group of congenital myopathies, characterized by the presence of distinct rod-like inclusions "nemaline bodies" in the sarcoplasm of skeletal muscle fibers. To date, *ACTA1*, *NEB*, *TPM3*, *TPM2*, *TNNT1*, and *CFL2* have been found to cause NM. We have identified recessive *RYR1* mutations in a patient with severe congenital NM, through high-throughput screening of congenital myopathy/muscular dystrophy-related genes using massively parallel sequencing with target gene capture. The patient manifested fetal akinesia, neonatal severe hypotonia with muscle weakness, respiratory insufficiency, swallowing disturbance, and ophthalomoplegia. Skeletal muscle histology demonstrated nemaline bodies and small type 1 fibers, but without central cores or minicores. Congenital myopathies, a molecularly, histopathologically, and clinically heterogeneous group of disorders are considered to be a good candidate for massively parallel sequencing.

Key words: nemaline myopathy (NM); massively parallel sequencing; the ryanodine receptor type 1 gene (*RYR1*); fetal akinesia; ophthalomoplegia

How to Cite this Article:
Kondo E, Nishimura T, Kosho T, Inaba Y, Mitsuhashi S, Ishida T, Baba A, Koike K, Nishino I, Nonaka I, Furukawa T, Saito K. 2012. Recessive *RYR1* mutations in a patient with severe congenital nemaline myopathy with ophthalomoplegia identified through massively parallel sequencing.
Am J Med Genet Part A 158A:772–778.

INTRODUCTION

Nemaline myopathy (NM) constitutes a group of congenital myopathies, characterized by the presence of distinct rod-like inclusions "nemaline bodies" in the sarcoplasm of skeletal muscle fibers. NM is clinically classified into six forms: severe congenital form, Amish NM, intermediate congenital form, typical congenital form, childhood-onset form, and adult-onset form. Severe congenital NM presents at birth with severe hypotonia and muscle weakness, little spontaneous movement, difficulties in sucking and

Additional supporting information may be found in the online version of this article.

Grant sponsor: Research Committee of Spinal muscular atrophy (SMA); Grant sponsor: Support Center for Women's Health Care Professionals and Researchers; Grant sponsor: Research on Intractable Diseases, Ministry of Health, Labour and Welfare, Japan; Grant sponsor: Ministry of Education, Culture, Sports, Science and Technology in Japan.

Eri Kondo and Takafumi Nishimura contributed equally to this work.

*Correspondence to:
Kayoko Saito, M.D., Ph.D., Institute of Medical Genetics, Tokyo Women's Medical University, 10-22 Kawada-cho, Shinjuku-ku, Tokyo 162-0054, Japan. E-mail: saito@img.twmu.ac.jp
**Correspondence to:
Tomoki Kosho, M.D., Department of Medical Genetics, Shinshu University School of Medicine, 3-1-1 Asahi, Matsumoto 390-8621, Japan. E-mail: ktomoki@shinshu-u.ac.jp

Published online 9 March 2012 in Wiley Online Library (wileyonlinelibrary.com).
DOI 10.1002/ajmg.a.35243

swallowing, gastroesophageal reflux, and respiratory insufficiency. Decreased fetal movements, polyhydramnios, and intrauterine death could occur. Early mortality is common, usually resulting from respiratory insufficiency or aspiration pneumonia, though occasional patients could survive long-term. To date, six genes have been found to cause NM: *ACTA1* (OMIM 102610), *NEB* (OMIM 161650), *TPM3* (OMIM 191030), *TPM2* (OMIM 190990), *TNNT1* (OMIM 191041), and *CFL2* (OMIM 601443) [North and Ryan, 2010]. *ACTA1* mutations are reported to account for roughly half of cases with severe congenital NM [Agrawal et al., 2004].

In this study, we report on a patient with severe congenital NM, characterized clinically by persistent ophthalomoplegia and histologically by small type 1 fibers in addition to nemaline bodies, but without central cores or minicores. Massively parallel sequencing of congenital myopathy/muscular dystrophy-related genes successfully identified compound heterozygous mutations in the ryanodine receptor type 1 gene (*RYR1*) (OMIM 180901).

CLINICAL REPORT

We investigated a now 2-year-old boy, clinically and histologically diagnosed with severe congenital NM. He is the first child of a healthy non-consanguineous Japanese couple with no family history of neuromuscular disorders. The fetal period had been complicated by nuchal translucency, fetal akinesia, and massive polyhydramnios. He was delivered at 35 weeks of gestation by vaginal vacuum extraction, with an Apgar score of 1 at 1 min. His birth weight was 2,048 g (−0.8SD), length 45 cm (−0.2SD), and head circumference 34 cm (+1.3SD). He showed severe generalized hypotonia, muscle weakness, central cyanosis, and bradycardia. After resuscitation with intratracheal intubation for severe apnea, he was admitted to the neonatal intensive care unit. He had a narrow face with facial muscle weakness, a high palate, reduced mouth opening, and mild bilateral blepharoptosis and ophthalmoplegia (Fig. 1a). On an appropriate ventilatory support, severe generalized muscle weakness and hypotonia persisted with a frog-leg posture and poor anti-gravity movements of the limbs (Fig. 1b). Extension of the elbows and knees were mildly limited. Micropenis, hypoplastic scrotum, and bilateral cryptorchidism were present. After tube feeding was started on the second day of birth, chylothorax occurred, requiring temporary intravenous nutrition. Serum creatine kinase and aldolase levels were normal. Nerve conduction studies showed normal velocities, amplitudes, and latencies. Electromyography showed myopathic changes (Fig. 2a).

He showed severe growth retardation in infancy. He had tracheotomy at age 6 months and gastrostomy with Nissen fundoplication at age 1 year. His height and weight caught up to normal ranges (Fig. 2b). From age 1 year, he gradually began moving his upper and lower extremities against gravity and the joint contractures improved, but proximal muscle weakness was still pronounced. He had no difficulties in opening his eyes, but no ocular movement was observed. He showed no swallowing

FIG. 1. a,b: Clinical photographs at age 2 weeks, showing a narrow face with facial muscle weakness and severe generalized muscle weakness and hypotonia. c,d: Clinical photographs at age 1 year 9 months. Patient shows an expressive face (c). He is polishing the teeth by himself (d).

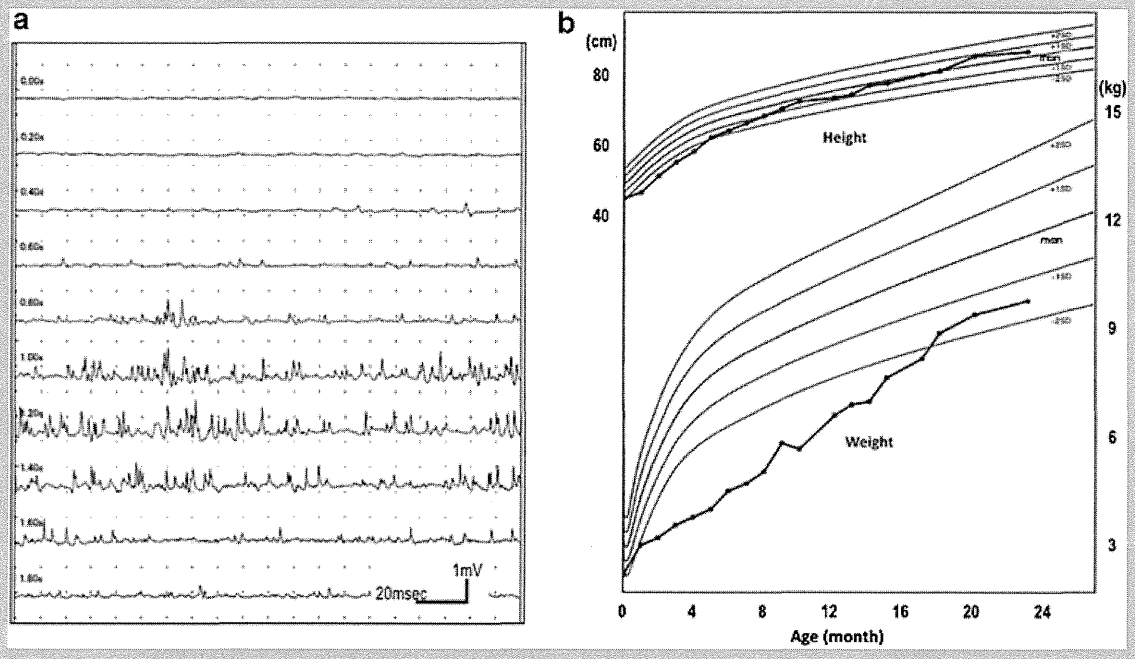

FIG. 2. a: Electromyography at age 2 months showing no abnormal insertion or resting discharges, but lower amplitudes and shorter durations in contraction. b: Growth curve showing both height and weight, delayed in infancy, catching up to normal ranges.

movement. He reached for an object at age 14 months, grasped an object at 16 months, and rolled over at 18 months. Social development was also observed, such as imitating his mother's hand movements at age 14 months and playing "peek-a-boo" at 16 months. When last seen by us at age 1 year and 9 months, he showed an expressive face and an active limb movement (Fig. 1c,d), though he was mechanically ventilated and could not sit or speak. He had no serious complications such as severe infections, cardiopulmonary dysfunction, scoliosis, or other neurological complications. Electroencephalography showed normal basic activities without paroxysmal discharges, and brain magnetic resonance image showed a mild myelination delay without structural abnormalities.

Muscle biopsy was obtained from the quadriceps at age 4 months. Specimens were immediately frozen and processed according to standard methods. The main pathological feature was nemaline bodies observed in the cytoplasm, but not in the nuclei (Fig. 3c); which were confirmed by electron microscopy (Fig. 4a,b). Additional features included very small type 1 fibers without central nuclei, fiber degeneration, or cellular infiltration (Fig. 3a, b, and d). Type 1 fibers were predominant, accounting for 71% of the total fiber number. Type 1 fibers were smaller than type 2 fibers by 34%, with the mean type 1 fiber diameter as $10.6 \pm 4.02\,\mu m$ (±SD) and with the mean type 2A fiber diameter as $16.1 \pm 5.17\,\mu m$ (±SD). Type 2B fibers were not detected, although there were a few Type 2C fibers. Neither the peripheral halo phenomenon nor central cores or minicores were observed (Fig. 3).

MATERIALS AND METHODS

Patients

The parents of the patient gave written informed consent for this study. The study was approved by the Ethics Committees of Tokyo Women's Medical University, Tokyo, Japan; and conformed to the guidelines involving human research as stated in the Declaration of Helsinki.

Targeted Capture and Next-Generation DNA Sequencing

Genomic DNA was extracted from peripheral blood leukocytes of the patient and his parents, using standard procedures. To identify disease-causing mutations, we used high-throughput screening system of congenital myopathies/muscular dystrophies-related genes through massively parallel sequencing with target gene capture, which we had established. The target gene capture was performed using the SureSelect™ Target Enrichment System (Agilent Technologies, CA). A custom set of SureSelect™ in-solution baits were designed using the eArray tool (http://www.opengenomics.com/earray) for capture of non-contiguous target muscle disease genomic regions approximately 3 Mb in total length, including *DMD* (OMIM 310200), *FKTN* (OMIM 607440), *LAMA2* (OMIM 156225), *DAG1* (OMIM 128239), *POMGNT1* (OMIM 606822), *POMT1* (OMIM 607423), *POMT2* (OMIM 607439), *TPM3, NEB, ACTA1, TPM2, TNNT1* (OMIM 191041),

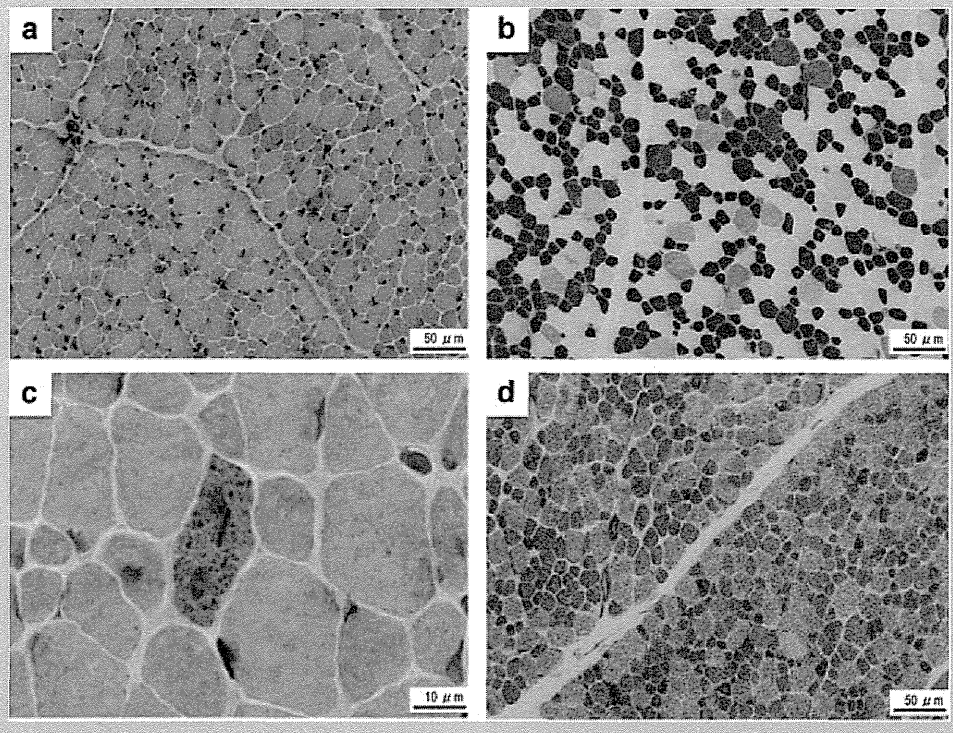

FIG. 3. Histopathological findings of skeletal muscle biopsy specimens. a: Hematoxylin–eosin staining showing fiber size variability without any dystrophic changes or inflammatory cell infiltrations. b: ATPase staining showing atrophic changes of type 1 fibers (dark stain) and decreased numbers of type 2B fibers (light stain). c: Modified Gomori trichrome staining showing nemaline bodies in the cytoplasm. d: NADH-TR staining showing type 1 fibers (dark stain) smaller than type 2 fibers (light stain). Bars indicate 50 μm (a, b, and d) or 10 μm (c).

CFL2 (OMIM 601443), *MTM1* (OMIM 300415), and *RYR1*. Then, 3 μg of the patient's genomic DNA was used for construction of a library composed of adaptor-ligated randomly fragmented DNA using the SOLiD Fragment Library Construction Kit (Applied Biosystems, CA) according to the manufacturer's instructions. The adaptor-ligated DNA was captured by hybridization in solution to the custom-designed cRNA oligonucleotide baits following the manufacturer's protocols. The enriched library DNA was sequenced using a SOLiD™ 4 System (Applied Biosystems) according to the manufacturer's instructions. The reads from each library were aligned against human genome sequence hg19 using Bioscope software (Applied Biosystems).

Validation of Mutations by Sanger Sequencing

For validation of detected variants, Sanger sequencing was performed. Primers were designed to amplify the detected novel missense mutations flanking sequence of *RYR1*. The amplification products were purified, directly sequenced with the BigDye terminator v3.1 Cycle Sequencing Kit (Applied Biosystems), and analyzed on a 3130×l genetic analyzer (Applied Biosystems).

RESULTS

More than 3,600 sequence variants were detected. Among them, we identified two non-synonymous single nucleotide substitutions in *RYR1*. These were heterozygous novel missense variants: c.4718 C > T (p.1573 Pro > Leu) in exon 33 and c.7585 G > A (p.2529 Asp > Asn) in exon 47. The nomenclature was based on the reference sequence *RYR1* (GenBank reference sequence, NM_000540.2), with nucleotide number 1 corresponding to the first base of the translation initiation codon. Sanger sequencing confirmed the variants and showed the parents to be heterozygous for each variant (Fig. 5). Neither of the variants was seen in 50 normal Japanese control samples, in 1000 Genomes Project data (http://www.1000genomes.org/data), or in the Exome Variant Server (EVS) Database (http://snp.gs.washington.edu/EVS/).

DISCUSSION

The patient we have described was clinically categorized into a severe congenital type of NM based on the clinical manifestations and histopathological findings, characterized by nemaline rods without central cores or minicores. Smallness of type 1 fibers, which is a non-specific common finding in many congenital